Journal of Sol-Gel Science and Technology (2022) 104:470–477
https://doi.org/10.1007/s10971-022-05890-1

INVITED PAPER: FUNCTIONAL COATINGS, THIN FILMS AND MEMBRANES (INCLUDING DEPOSITION TECHNIQUES)

Preparation of polyacrylamide-silica organic-inorganic hybrid membranes for carbon dioxide separation via in-situ polymerization

Koji Kuraoka[1,2] · Ryoga Yamamoto[1]

Received: 28 February 2022 / Accepted: 22 June 2022 / Published online: 14 July 2022

Abstract

Polyacrylamide (PAAm)-silica organic-inorganic hybrid membranes for carbon dioxide (CO_2) separation were prepared via in-situ polymerization. Formation of silica and PAAm via sol-gel method and in-situ polymerization was confirmed by IR spectroscopy. Single gas permeances through the membranes were measured at 298, 373 and 423 K using CO_2, He and N_2. The ideal separation factor (the ratio of the permeances) of CO_2/N_2 through the AAm10 membrane (starting solution composition; tetraethoxysilane: methyltriethoxysilane: distilled water: hydrochloric acid: ethanol: acrylamide: dimethyl 2,2′-azobis(isobutyrate) = 0.4: 0.6: 2: 0.01: 20: 1.0: 0.1 in molar ratio) was 25.4 at 298 K. This value was thirty times higher than the theoretical Knudsen value ($CO_2/N_2 = 0.8$). Binary gas permeation at 298 K was also investigated using a gas mixture of 50%CO_2–50%N_2. The ideal separation factor (the ratio of the permeances) of CO_2/N_2 through the membrane was 24.9. This value was the same as the ideal separation factor of CO_2/N_2 calculated from the single gas measurement. Such a high CO_2 selectivity in 50%CO_2-50%N_2 feed gas was also found even at high temperature for this membrane.

Graphical abstract

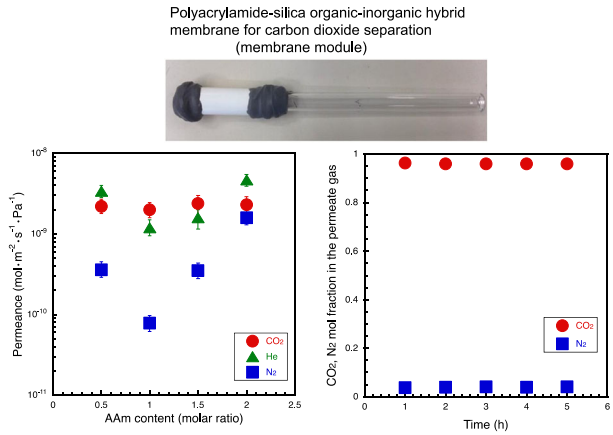

Keywords Polyacrylamide · Silica · Organic-inorganic hybrid · Carbon dioxide · Separation membrane · In-situ polymerization

✉ Koji Kuraoka
kuraoka@maritime.kobe-u.ac.jp

[1] Graduate School of Maritime Sciences, Kobe University, 5-1-1 Fukaeminami, Higashinada, Kobe 658-0022, Japan

[2] Research Center for Membrane and Film Technology, Kobe University, 1-1 Rokkodai, Nada, Kobe 657-8501, Japan

Highlights

- Polyacrylamide-silica organic-inorganic hybrid membranes for carbon dioxide (CO_2) separation were prepared via in-situ polymerization.
- The effects of acrylamide (AAm) content on the gas permeances of CO_2, He, N_2 through the membranes were investigated.
- AAm10 membrane (starting solution composition; tetraethoxysilane: methyltriethoxysilane: distilled water: hydrochloric acid: ethanol: acrylamide: dimethyl 2,2′-azobis(isobutyrate) = 0.4:0.6:2:0.01:20:1.0:0.1 in molar ratio) exhibits the highest CO_2 selectivity, the ideal separation factor (the ratio of the permeances) of CO_2/N_2 was 25.4 at 298 K.
- AAm10 membrane exhibited high CO_2 selectivity at 298 K for 50%CO_2-50%N_2 feed gas mixture, where the ideal separation factor (the ratio of the permeances) of CO_2/N_2 was 24.9.

1 Introduction

Exponentially rising global emissions of greenhouse gases, especially carbon dioxide (CO_2), are the source of global warming and climate change. A report from the Intergovernmental Panel on Climate Change (IPCC) states that atmospheric levels of CO_2 will rise to about 450 ppm by the years 2021~40 and global temperatures will rise by 1.5 °C [1]. Increased amounts of CO_2 are believed to be the main reasons for increased surface temperatures, which result in intense heat waves, droughts, temperature changes, sea level rise, and glacier melting [2]. In recent years, agreements, such as the Paris Agreement and the Kyoto Protocol, have been signed to regulate and reduce CO_2 emissions around the world. Carbon dioxide Capture, Utilization and Storage (CCUS) is being developed worldwide to regulate and reduce CO_2 emissions. Membrane separation is drawing attention in the CO_2 separation process in CCUS [3].

Compared to traditional adsorption methods, membrane separation is a low energy process for the physical separation of CO_2 because it does not involve the use of thermal energy nor the need for phase transition. The application of CO_2 separation membranes ranges from biogas refining [4], hydrogen production [5], natural gas refining [6, 7], CCUS [3], and membrane separation has proven cost-efficient and it has shown excellent environmental results. Existing CO_2 separation membranes are the mixed matrix membranes [8, 9], the metal organic framework membranes [10], the carbon molecular sieve membranes [11, 12], the zeolite membranes [13–15], the inorganic membranes [16, 17] and the polymer membranes [18, 19].

Furthermore, a large variety of organic-inorganic hybrid membranes for gas separation have been reported, such as organic-inorganic hybrid membranes prepared from hydroxyl-terminated polyether and 3-isocyanatopropyltriethoxysilane for CO_2 separation [20], organic-inorganic hybrid silica membranes with controlled silica network size for hydrogen (H_2) separation [21], polyetheramine–polyhedral oligomeric silsesquioxane organic-inorganic hybrid membranes for CO_2 separation [22], silica and novel functionalized silica-based cellulose acetate hybrid membranes for nitrogen (N_2) separation [23], a hydrostable mesoporous γ-Al_2O_3 membrane modified with Si–C–H organic-inorganic hybrid derived from polycarbosilane for H_2 separation [24], reduced graphene oxide/organosilica hybrid membrane for H_2 and CO_2 separation [25]. For silica-polyacrylamide (PAAm) hybrids, in literature, mesoporous hybrid silica-PAAm aerogels and xerogels were prepared by sol-gel method [26]. PAAm-based hydrogels containing 3-(trimethoxysilyl)propyl methacrylate and/or tetraethoxysilane were synthesized by means of frontal polymerization using ammonium persulfate as initiator, N,N′-methylene bisacrylamide as crosslinking agent and dimethyl sulfoxide as solvent [27], and silica/PAAm nanocomposite as a steel anticorrosive layer was prepared using dispersion radical polymerization technique [28]. Silica-PAAm nanocomposite films for moisture separation were prepared by radical polymerization using acrylamide, bis-acrylamide, aqueous dispersion of spherical silica nanoparticles [29]. Organic/inorganic hybrid composed of modified PAAm grafted silica supported Pd nanoparticles for a catalyst was prepared by reversible addition-fragmentation chain transfer polymerization [30], and highly hydrophilic organic/inorganic composite hydrogels based on PAAm and silica were prepared by in-situ polymerization using acrylamide and sodium silicate in aqueous solution [31]. The reported PAAm-silica hybrids and composites have been applied to mesoporous aerogel, xerogel, hydrogel, anticorrosive layer, films for moisture separation and catalysts.

However, there are no reports on the preparation of PAAm-silica organic-inorganic hybrid membranes for CO_2 separation and the investigation of CO_2 permeation and separation properties.

In this study, we report PAAm-silica organic-inorganic hybrid membranes for CO_2 separation prepared by in-situ polymerization.

Amine compounds are well-known for CO_2 absorption ability and they have been used in CO_2 absorption solution of CO_2 separation and recovery apparatus. In addition, amino functional group is also known as a functional group with CO_2 affinity. It has thus been used as CO_2 carrier in a facilitated CO_2 transport membrane [32]. However, it is

difficult to control the CO_2 affinity and to fix a large amount of it in the membrane due to low solubility of polymer in the coating solution. We propose sol-gel method and in-situ polymerization using silicon alkoxide and acrylamide monomer to solve these problems. PAAm is synthesized by in-situ polymerization during sol-gel reaction of silicon alkoxide, and is fixed in the silica network. To use in-situ polymerization, it can introduce a large amount of PAAm in the hybrid membrane because of higher solubility of monomer in the coating solution than polymer. Based on this concept, we have prepared a novel organic-inorganic hybrid membrane for CO_2 separation.

2 Experimental

PAAm-SiO_2 organic-inorganic hybrid membranes for CO_2 separation were prepared via in-situ polymerization. Sols were composed of tetraethoxysilane (TEOS, Kanto Chemical Co., Inc.), methyltriethoxysilane (MeTEOS, Shin-Etsu Chemical Co., Ltd.), distilled water (H_2O), hydrochloric acid (HCl, Kanto Chemical Co., Inc.), ethanol (EtOH, Kanto Chemical Co., Inc.), acrylamide (AAm, Tokyo Chemical Industry Co., Ltd.) and dimethyl 2,2′-azobis(isobutyrate) (V-601, FUJIFILM Wako Pure Chemical Corporation) as radical polymerization initiator. Table 1 shows the starting solution composition of the prepared membranes and sample names. Commercially available reagent grade chemicals were used. AAm was added to a mixture of EtOH, H_2O and HCl at room temperature. After stirring for 30 min, TEOS was introduced into the mixture and the resulting mixture was stirred for 1 h. Then MeTEOS was added to the mixture and stirring for 1 h. Afterwards, V-601 was added to the mixture and it was stirred for another 1 h at room temperature to obtain a homogeneous sol. The prepared sol was clear and homogeneous.

The intermediate layer was prepared by dip coating using a commercial silica colloid, Snowtex O (particle size of 10–20 nm, Nissan Chemical Industries., Ltd). The compositions of silica colloid sols for dip-coating were Snowtex O: EtOH = 1:10 (Sol A) and 1:15 (Sol B) in mass ratio. Porous alumina tubes (Iwao Jiki Kogyo Co., Ltd.) with a mean pore diameter of 0.1 μm, an outer diameter of 12 mm, an inner diameter of 9 mm and a length of 5 cm were used as the supports. The supports were dipped in the sol, before being withdrawn at a rate of 1 mm/s, and then dried at room temperature. The dip coating process was repeated twice, and then the membranes were heated to 873 K at a rate of 2 K/min, and maintained at the maximum temperature for 2 h, before being cooled down to room temperature at the rate of 2 K/min. These coating and heating procedures were repeated twice (Sol A at first and then Sol B) following the same protocol.

Table 1 Sample name and starting solution composition

Sample	Starting solution composition (molar ratio)						
	TEOS	MeTEOS	H_2O	HCl	EtOH	AAm	V-601
AAm05	0.4	0.6	2	0.01	20	0.5	0.05
AAm10						1.0	0.10
AAm15						1.5	0.15
AAm20						2.0	0.20

The membranes prepared by this process were then used as a support for the preparation of organic-inorganic hybrid membranes for CO_2 separation. The supports were dipped in the sol as shown in Table 1, and withdrawn at a rate of 1 mm/s, and then dried at 338 K for 1 h. After repeating the dip coating procedure twice, the membranes were heated at 423 K for 2 h in the air with a heating and cooling rate of 0.5 K/min. These dip coating and heating procedures were repeated twice in a similar manner to obtain the membranes.

After drying at 373 K in a vacuum oven, single gas permeance through the membranes were measured at 298 K (room temperature) 373 K and 423 K using CO_2, He and N_2 with the same procedure as described previously [33]. One end of the tubular membrane was sealed, and the other was connected to a Pyrex glass tube with epoxy resin. The membrane modules were supported in a gas flow cell. Pressure differences of the gases through the membranes were kept at 1 atm (1.013×10^5 Pa) and the permeance measured using a mass flow meter (SEF-E40, HORIBA STEC, Co., Ltd.). The permeances were measured in the order of N_2, He, and CO_2 at constant temperature. The permeance measurements were done first at 298 K, then at 373 K and 423 K, and finally at 298 K, confirming membrane damage and reproducibility of the permeances. The final measurement at 298 K showed that the permeance was about the same as the permeance at the first 298 K, and this indicates that the high temperature measurement (at 423 K) did not damage the membrane. The single gas permeance was tested on three membranes and all error bars represent the average error of the three membranes prepared under the same conditions. The permeance was calculated by the flow rate, the membrane area, the pressure difference (1 GPU = 3.35×10^{-10} mol•m^{-2}•s^{-1}•Pa^{-1}). The ideal separation factor of CO_2/N_2 was calculated using the ratio of the CO_2 permeance to N_2 permeance.

To evaluate the CO_2 separation characteristics of the membrane, binary gas separation of the membrane was measured at 298 K using a gas mixture of 50%CO_2-50%N_2 as feed gas. The experimental apparatus was the same as described previously [33]. A membrane module prepared using the same procedure as described above was supported in a gas flow cell into which a gas mixture of 50%CO_2-50%

N_2 was applied. The pressure of the feed gas was kept at 2 atm (2.026×10^5 Pa). The gas compositions of the feed and the permeate gas were analyzed by gas chromatograph (GC-8A, Shimadzu Corporation) in combination with a thermal conductivity detector equipped with a column of Sunpak-A (column temperature of 333 K). The ideal separation factor of CO_2/N_2 was calculated from mole fraction of CO_2 in the feed and the permeate gas using the following equation [34].

$$\alpha = \frac{y_A}{1 - y_A} \times \frac{1 - x_A - \Phi(1 - x_A)}{x_A - \Phi y_A} \quad (1)$$

$$\Phi = \gamma + \theta - \gamma\theta \quad (2)$$

$$\gamma = \frac{P_l}{P_h} \quad (3)$$

$$\theta = \frac{F_p}{F_f} \quad (4)$$

where, x_A denotes the mole fraction of CO_2 in feed gas, y_A represents the mole fraction of CO_2 in permeate gas, Φ is the operating factor, γ the operating pressure ratio, θ denotes the cut, P_l represents the downstream pressure, P_h denotes upstream pressure, F_p represents flux of permeate, F_f is the flux of the feed.

3 Results and discussion

Single gas permeance for CO_2, He, N_2 through the membranes were measured at 298 K (room temperature) for AAm content are shown in Fig. 1. Since the errors of the permeances were not so large, the prepared membranes were considered homogeneous. The CO_2, He and N_2 permeance of AAm10 membrane was the lowest value. The N_2 permeance of the membranes decreased to AAm10 and then increased as the content of AAm increased. This is probably because PAAm was well dispersed in the silica network of AAm10 allowing it to develop a homogeneous dense structure without aggregation of PAAm and silica. Therefore, the lowest N_2 permeance was observed. The fact that N_2 adsorption was not observed in the N_2 adsorption measurement at 77 K is considered to be one of the evidences that AAm10 membrane has a dense structure. The N_2 permeance increase of AAm15 and AAm20 membrane thought to be due to defects in the membranes caused by aggregation of PAAm and silica. The defects were so small in size that they cannot be detected by SEM observation. It is difficult to specify the defects. The defects are expected to molecular spaces (like free volumes or pores) caused by imperfection of organic-inorganic hybridization (aggregates of PAAm or silica). For AAm10 membrane, the ideal separation factor of

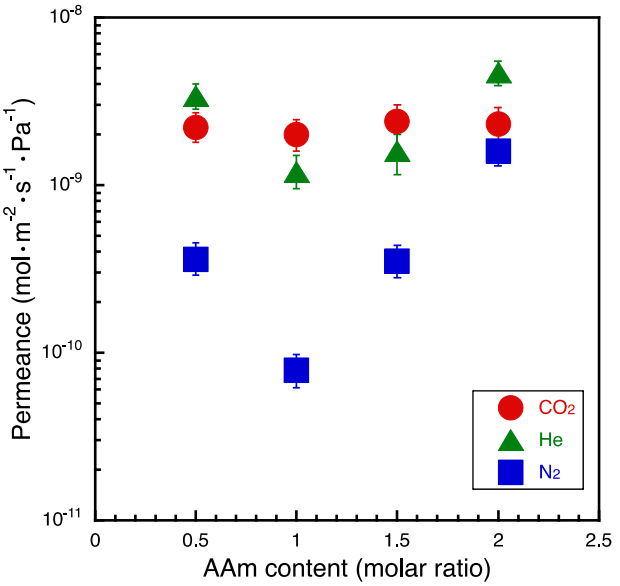

Fig. 1 Change in the permeances of CO_2, He, N_2 through the membranes at 298 K on AAm content

Table 2 Gas permeation data of porous alumina tube and porous alumina tube with intermediate layer

Sample	Permeance (mol•m^{-2}•s^{-1}•Pa^{-1})			Ideal separation factor	
	N_2	He	CO_2	He/N_2	CO_2/N_2
Porous alumina tube	2.0×10^{-5}	3.0×10^{-5}	2.9×10^{-5}	1.5	1.4
Porous alumina tube with intermediate layer (support)	8.5×10^{-7}	2.1×10^{-6}	7.2×10^{-7}	2.5	0.9

CO_2/N_2 was 25.4, and the CO_2 permeance was 6.0 GPU (2.0×10^{-9} mol•m•m^{-2}•s^{-1}•Pa^{-1}). Table 2 shows gas permeation data of a porous alumina tube and a porous alumina tube with intermediate layer (support). The CO_2 permeance through a porous alumina tube and through a porous alumina tube with intermediate layer (support) were 87,000 GPU (2.9×10^{-5} mol•m•m^{-2}•s^{-1}•Pa^{-1}) and 2100 GPU (7.2×10^{-7} mol•m•m^{-2}•s^{-1}•Pa^{-1}), respectively. By introducing the intermediate layer, the CO_2 permeance was reduced to ~1/40, and it can be seen that the intermediate layer has the resistance of gas permeance. From the ideal separation factor of CO_2/N_2 and He/N_2, the gas permeation through the support was predominantly governed by Knudsen flow. In addition, the CO_2 permeance through AAm10 membrane was ~350 times lower than that of the support, indicating that the resistance of gas permeance is very high. This higher resistance of gas permeation is considered to be due to a dense structure of AAm10 membrane and the apparent thickness of the membrane thickened by

penetration of the sol (precursor solution) into the pores of the support. The CO_2/N_2 selectivity of AAm10 membrane is ~30 times the theoretical Knudsen value ($CO_2/N_2 = 0.8$) and 2.5 times higher than the reported hybrid polydimethylsiloxane membranes [35]. However, the CO_2 permeance is ~4.5 times lower than that of the reported hybrid membrane (27.7 GPU) [35]. This high selectivity for CO_2 is thought to be due to the affinity of amino functional group for CO_2 in PAAm. The CO_2 permeance through AAm10 membrane was higher than that of He and N_2 as shown in Fig. 1. It is thus concluded that AAm10 membrane have a strong affinity for CO_2, which preferentially permeated through the membrane by the facilitated transport or solution-diffusion mechanisms.

Recently, Hasegawa et al. reported high-silica CHA-type zeolite membrane for CO_2 separation. The CO_2/N_2 selectivity of the membrane was ~10, and the CO_2 permeance through the membrane was ~1500 GPU ($\sim 5 \times 10^{-7}$ mol m^{-2} s^{-1} Pa^{-1}) at 303 K on single gas measurement [14]. For polymer membranes, the CO_2/N_2 selectivity and the CO_2 permeance of poly[bis(2-(2-methoxyethoxy) ethoxy) phosphazene] membrane was 62.5 and 2.5 GPU (8.4×10^{-10} mol m^{-2} s^{-1} Pa^{-1}), respectively [36, 37]. And those of cardo polymer (polyamide) membrane was 37 and 0.25 GPU (8.5×10^{-11} mol m^{-2} s^{-1} Pa^{-1}) [38]. Compared to AAm10 membrane, zeolite membrane exhibits high CO_2 permeance and low CO_2/N_2 selectivity due to exitance of the pores, and polymer membranes achieve high selectivity and low permeance due to dense (non-porous) membrane. Although AAm10 membrane was dense membrane, it showed relatively high selectivity and high CO_2 permeance.

The structures of the membranes were investigated by a Fourier transform infrared spectrometer (FT/IR-4100, JASCO Corporation). Figure 2 indicates IR spectra of AAm10 (with the best CO_2 selectivity), PAAm and AAm, from 4000 to 400 cm^{-1}. IR spectrum of AAm10 showed the characteristic bands related to Si-O-Si bond (~1220 and ~1080 cm^{-1}) and CH_3-Si (~1300 cm^{-1}), which confirm the sol-gel reaction of TEOS and MeTEOS [39]. Other characteristic bands originating from PAAm were also observed in AAm10. PAAm had two absorption bands at around 1700–1600 cm^{-1}, which correspond to the C=O stretching and NH_2 bending vibration [40]. The band at ~1660 cm^{-1} is due to the stretching band of C=O. Compared to that of Am, these bands in AAm10 and PAAm were shifted to lower wavenumbers indicating the existence of hydrogen bonding between C=O and Si-OH or NH_2 of PAAm [41]. Only AAm indicated other absorption bands from 2800 to 1900 cm^{-1}. The absorption at ~1920 cm^{-1} is due to overtone band of H_2C=C bending vibration, at ~2430 cm^{-1} corresponds to combination bands of NH_2 bending vibration and HRC=C bending vibrations, at ~2780 cm^{-1} is related to combination bands of C=C stretching vibration and NH_2 bending

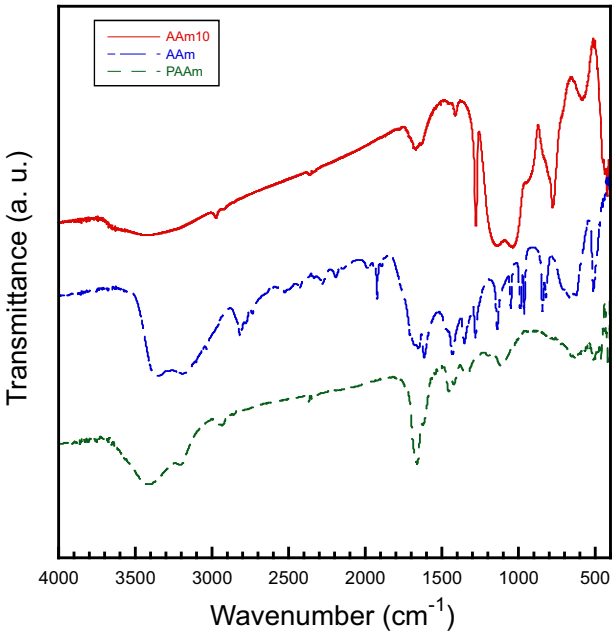

Fig. 2 IR spectra of the AAm10, AAm and PAAm

vibration and at ~2800 cm^{-1} is due to C-H stretching vibration [42]. Therefore, in AAm10, almost all parts of AAm were thought to exist as polymerized PAAm via in-situ polymerization. From the results, it was suggested that AAm10 had silica network and PAAm structure had formed from the sol-gel reaction and the in-situ polymerization.

SEM photograph of the outer surface (coating side) morphology of (a) the support (a porous alumina tube with the intermediate layer) and (b) the AAm10 membrane is shown in Fig. 3. The support surface was covered by the hybrid layer and no cracks were observed. However, there was little difference in surface morphology between (a) the support and (b) the AAm10 membrane. This suggests that the interface between the membrane and the support may be vague due to the membrane precursor solution penetration into the pores of the support. And the result supports the conclusion that the gas permeance through this membrane exhibited the lowest value.

Figure 4 indicates the permeances of CO_2, He and N_2 through the AAm10 membrane at 298, 373 and 423 K. The CO_2 and He permeances were 10^{-9} to 10^{-8}, and the N_2 permeances through the membrane were 10^{-11} to 10^{-9} mol•m^{-2}•s^{-1}•Pa^{-1}. The permeances through the membrane almost increased with the increase in temperature. N_2 permeance increased dramatically (almost 10 times) from 298 K to 373 K, but showed approximately the same value at 423 K. These permeances were reproducible. The reason of this behavior is not clear at this time. However, the N_2 permeance is thought to be governed by solution-diffusion mechanism [43], and the diffusion coefficient of N_2 in the membrane were high and the solubility coefficient of N_2 were low due to the high temperature. Only He permeance

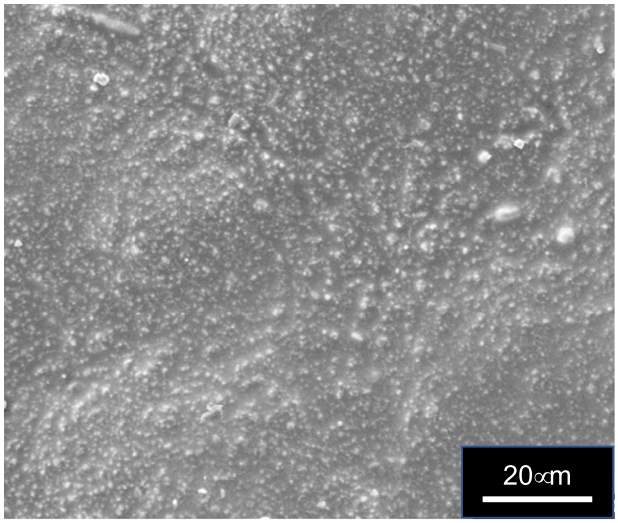

(a) The support

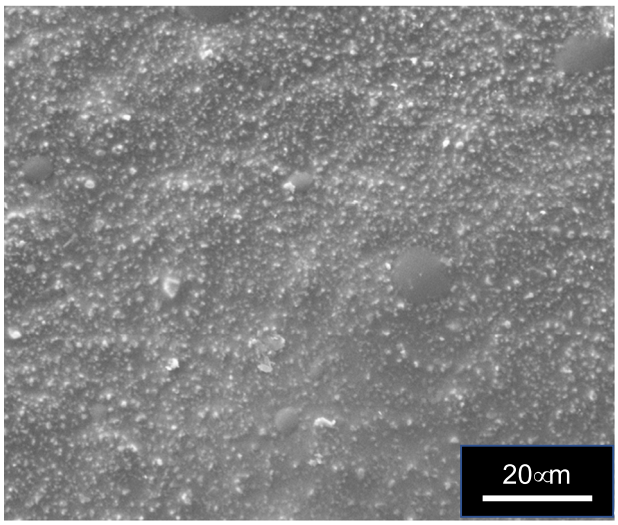

(b) The AAm membrane

Fig. 3 SEM photograph of the outer surface (coating side) morphology of (**a**) the support and (**b**) the AAm10 membrane

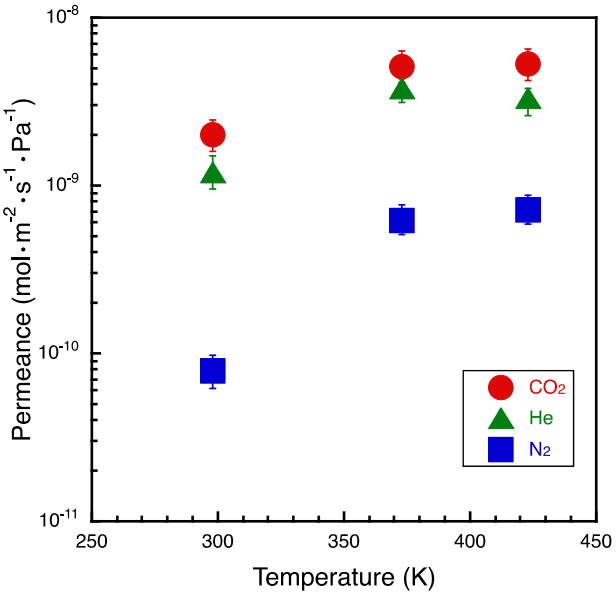

Fig. 4 The permeances of CO_2, He and N_2 through the AAm10 membrane at 298, 373 and 423 K

at 423 K was decreased due to lower solubility for He at high temperature. It was thus concluded that CO_2 permeation in this case is predominantly governed by facilitated transport mechanism (with fixed carriers) [44] and the permeation of other gases (He and N_2) is governed by solution-diffusion mechanism [43]. The AAm10 membrane are thought to be homogenously dispersed with amino functional group (-NH_2) of PAAm. The membrane thus has a dense structure with -NH_2 (PAAm), in which the facilitated transport mechanism (with fixed carriers) operates. Therefore, the CO_2 permeances through the membrane are higher than the N_2 permeances.

Binary gas separation of AAm10 membrane was measured at 298 K using a gas mixture of 50%CO_2-50%N_2 as feed gas to confirm the CO_2 separation property. Time dependence of the CO_2, N_2 mole fraction in the permeate gas is shown in Fig. 5. The N_2 mol fraction in the permeate gas was low (~0.04) during measuring time. In contrast, CO_2 mol fraction in the permeate gas was high (~0.96) and nearly constant for the duration of the experiment up to 5 h, implying that the activity of -NH_2 as CO_2 carriers is stable in this membrane. One of the main disadvantages of the polymeric membrane is plasticization when being used in high-pressure and high concentration of CO_2 as feed gas [45]. However, the prepared membrane (AAm10) exhibited high CO_2 selectivity even at a pressure as high as 2 atm and at a feed gas CO_2 concentration as high as 100%, which may be due to its mechanical toughness of the organic-inorganic hybrid structure. The ideal separation factor of CO_2/N_2 was calculated from mole fraction of CO_2 in the feed gas and the permeate gas. CO_2 in the gas mixture (50%) was concentrated to more than 95% by using AAm10 membrane at 298 K. The ideal separation factor of CO_2/N_2 through the membrane was 24.9. This value was almost the same as the CO_2/N_2 selectivity factor calculated from the single gas measurement ($CO_2/N_2 = 25.4$). From this result, the AAm10 membrane also indicated high CO_2 selectivity in binary gas separation.

4 Conclusion

The PAAm-silica organic-inorganic hybrid membranes for CO_2 separation were prepared by in-situ polymerization. The CO_2, He and N_2 permeances through the hybrid

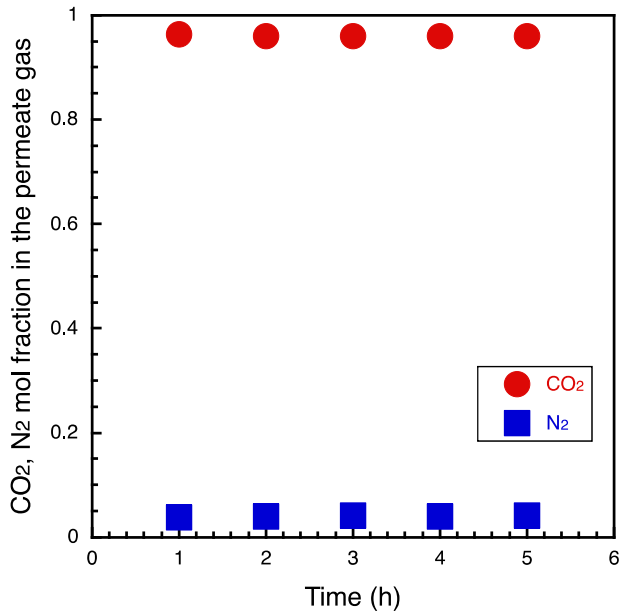

Fig. 5 Time dependence of the CO_2, N_2 mole fraction in the permeate gas

membranes were evaluated as the function of acrylamide (AAm) content. The ideal separation factor of CO_2/N_2 for AAm10 (starting solution composition; TEOS: MeTEOS: H_2O:HCl:EtOH: AAm: V-601 = 0.4:0.6:2:0.01:20:1.0:0.1 in molar ratio) membrane was the highest value ($CO_2/N_2 = 25.4$). This membrane presents CO_2-selectivity even at relatively high temperature as well as at 298 K for a gas mixture of 50%CO_2-50%CO_2 (the ideal separation factor of $CO_2/N_2 = 24.9$ at 298 K).

Author contributions All authors contributed to the study conception and design. Material preparation, data collection and analysis were performed by KK and RY. The first draft of the manuscript was written by KK and all authors commented on previous versions of the manuscript. All authors read and approved the final manuscript.

Funding This work was supported by JSPS KAKENHI Grant Number JP19K12397.

Compliance with ethical standards

Conflict of interest The authors declare no competing interests.

Publisher's note Springer Nature remains neutral with regard to jurisdictional claims in published maps and institutional affiliations.

References

1. Masson- Delmotte V, Zhai P, Pirani A, Connors SL, Péan C, Berger S, Caud N, Chen Y, Goldfarb L, Gomis MI, Huang M, Leitzell K, Lonnoy E, Matthews JBR, Maycock TK, Waterfield T, Yelekçi O, Yu R, Zhou B (in Press) IPCC, 2021: Summary for Policymakers. In: Climate Change 2021: The Physical Science Basis. Contribution of Working Group I to the Sixth Assessment Report of the Intergovernmental Panel on Climate Change.
2. Ahmed R, Liu G, Yousaf B, Abbas Q, Ullah H, Ali MU (2020) Recent advances in carbon-based renewable adsorbent for selective carbon dioxide capture and separation-A review. J Clean Prod 242:118409. https://doi.org/10.1016/j.jclepro.2019.118409
3. Míguez JL, Porteiro J, Pérez-Orozco R, Gómez MÁ (2018) Technology Evolution in Membrane-Based CCS. Energies 11 (11). https://doi.org/10.3390/en11113153
4. Baena-Moreno FM, le Saché E, Pastor-Pérez L, Reina TR (2020) Membrane-based technologies for biogas upgrading: a review. Environ Chem Lett 18(5):1649–1658. https://doi.org/10.1007/s10311-020-01036-3
5. Gouveia ASL, Ventaja L, Tomé LC, Marrucho IM (2018) Towards Biohydrogen Separation Using Poly(Ionic Liquid)/Ionic Liquid Composite Membranes. Membranes 8 (4). https://doi.org/10.3390/membranes8040124
6. Scholes CA, Stevens GW, Kentish SE (2012) Membrane gas separation applications in natural gas processing. Fuel 96:15–28. https://doi.org/10.1016/j.fuel.2011.12.074
7. Hazazi K, Ma X, Wang Y, Ogieglo W, Alhazmi A, Han Y, Pinnau I (2019) Ultra-selective carbon molecular sieve membranes for natural gas separations based on a carbon-rich intrinsically microporous polyimide precursor. J Membr Sci 585:1–9. https://doi.org/10.1016/j.memsci.2019.05.020
8. Wong KK, Jawad ZA (2019) A review and future prospect of polymer blend mixed matrix membrane for CO_2 separation. J Polym Res 26(12):289. https://doi.org/10.1007/s10965-019-1978-z
9. Ahmad NNR, Leo CP, Mohammad AW, Shaari N, Ang WL (2021) Recent progress in the development of ionic liquid-based mixed matrix membrane for CO_2 separation: A review. Int J Energy Res 45(7):9800–9830. https://doi.org/10.1002/er.6518
10. Venna SR, Carreon MA (2015) Metal organic framework membranes for carbon dioxide separation. Chem Eng Sci 124:3–19. https://doi.org/10.1016/j.ces.2014.10.007
11. Kumar R, Zhang C, Itta AK, Koros WJ (2019) Highly permeable carbon molecular sieve membranes for efficient CO_2/N_2 separation at ambient and subambient temperatures. J Membr Sci 583:9–15. https://doi.org/10.1016/j.memsci.2019.04.033
12. Lei L, Lindbråthen A, Zhang X, Favvas EP, Sandru M, Hillestad M, He X (2020) Preparation of carbon molecular sieve membranes with remarkable CO_2/CH_4 selectivity for high-pressure natural gas sweetening. J Membr Sci 614:118529. https://doi.org/10.1016/j.memsci.2020.118529
13. Tomita T, Nakayama K, Sakai H (2004) Gas separation characteristics of DDR type zeolite membrane. Microporous Mesoporous Mater 68(1):71–75. https://doi.org/10.1016/j.micromeso.2003.11.016
14. Hasegawa Y, Abe C, Natsui M, Ikeda A (2021) Gas permeation properties of high-silica CHA-type zeolite membrane. Membranes 11 (4). https://doi.org/10.3390/membranes11040249
15. Cao Z, Anjikar ND, Yang S (2022) Small-pore zeolite membranes: a review of gas separation applications and membrane preparation. Separations 9 (2). https://doi.org/10.3390/separations9020047
16. Kuraoka K, Tanaka H, Yazawa T (1996) Highly selective separation of CO_2 and He by xerogel coated porous glass membrane. J Mater Sci Lett 15(1):1–3. https://doi.org/10.1007/BF01855593
17. Pera-Titus M (2014) Porous inorganic membranes for CO_2 capture: present and prospects. Chem Rev 114(2):1413–1492. https://doi.org/10.1021/cr400237k
18. Sridhar S, Smitha B, Aminabhavi TM (2007) Separation of carbon dioxide from natural gas mixtures through polymeric membranes—a review. Sep Purif Rev 36(2):113–174. https://doi.org/10.1080/15422110601165967
19. Russo F, Galiano F, Iulianelli A, Basile A, Figoli A (2021) Biopolymers for sustainable membranes in CO_2 separation: a

review. Fuel Process Technol 213:106643. https://doi.org/10.1016/j.fuproc.2020.106643
20. Kim H, Lim C, Hong S-I (2005) Gas permeation properties of organic-inorganic hybrid membranes prepared from hydroxyl-terminated polyether and 3-isocyanatopropyltriethoxysilane. J Sol-Gel Sci Technol 36(2):213–221. https://doi.org/10.1007/s10971-005-3782-y
21. Kanezashi M, Yada K, Yoshioka T, Tsuru T (2010) Organic–inorganic hybrid silica membranes with controlled silica network size: Preparation and gas permeation characteristics. J Membr Sci 348(1):310–318. https://doi.org/10.1016/j.memsci.2009.11.014
22. Chua ML, Shao L, Low BT, Xiao Y, Chung T-S (2011) Polyetheramine–polyhedral oligomeric silsesquioxane organic–inorganic hybrid membranes for CO_2/H_2 and CO_2/N_2 separation. J Membr Sci 385-386:40–48. https://doi.org/10.1016/j.memsci.2011.09.008
23. Minhas FT, Farrukh S, Hussain A, Mujahid M (2015) Comparison of silica and novel functionalized silica-based cellulose acetate hybrid membranes in gas permeation study. J Polym Res 22(4):63. https://doi.org/10.1007/s10965-015-0701-y
24. Kubo M, Kojima M, Mano R, Daiko Y, Honda S, Iwamoto Y (2020) A hydrostable mesoporous γ-Al_2O_3 membrane modified with Si–C–H organic-inorganic hybrid derived from polycarbosilane. J Membr Sci 598:117799. https://doi.org/10.1016/j.memsci.2019.117799
25. Zhao Y, Zhou C, Kong C, Chen L (2021) Ultrathin reduced graphene oxide/organosilica hybrid membrane for gas separation. JACS Au 1(3):328–335. https://doi.org/10.1021/jacsau.0c00073
26. Ramadan H, Coradin T, Masse S, El-Rassy H (2011) Synthesis and characterization of mesoporous hybrid silica-polyacrylamide aerogels and xerogels. Silicon 3(2):63–75. https://doi.org/10.1007/s12633-010-9064-5
27. Illescas J, Sanna R, Alzari V, Nuvoli D, Casu M, Sanna R, Rivera E, Mariani A (2013) Organic–inorganic interpenetrating polymer networks and hybrid polymer materials prepared by frontal polymerization. J Polym Sci A: Polym Chem 51(21):4618–4625. https://doi.org/10.1002/pola.26882
28. El-Mahdy GA, Atta AM, Al-Lohedan HA, Tawfik AM, Abdel-Khalek AA (2015) Application of Silica/polyacrylamide nanocomposite as Anticorrosive layer for Steel. Int J Electrochem Sci 10(1):151–161
29. Mirbagheri M, Hill RJ (2017) Sorption and diffusion of moisture in silica-polyacrylamide nanocomposite films. Polymer 122:359–371. https://doi.org/10.1016/j.polymer.2017.04.071
30. Ghasemi S, Karim S (2018) Organic/inorganic hybrid composed of modified polyacrylamide grafted silica supported Pd nanoparticles using RAFT polymerization process: Controlled synthesis, characterization and catalytic activity. Mater Chem Phys 205:347–358. https://doi.org/10.1016/j.matchemphys.2017.11.041
31. Slisenko O, Mamunya Y (2019) Novel highly hydrophilic organic/inorganic composites based on polyacrylamide and silica: synthesis strategy, structure and swelling behaviour. J Polym Res 26(7):164. https://doi.org/10.1007/s10965-019-1823-4
32. Tong Z, Ho WSW (2017) Facilitated transport membranes for CO_2 separation and capture. Sep Sci Technol 52(2):156–167. https://doi.org/10.1080/01496395.2016.1217885
33. Kuraoka K, Kubo N, Yazawa T (2000) Microporous silica xerogel membrane with high selectivity and high permeance for carbon dioxide separation. J Sol-Gel Sci Technol 19(1):515–518. https://doi.org/10.1023/A:1008728320293
34. Kuraoka K, Chujo Y, Yazawa T (2001) Hydrocarbon separation via porous glass membranes surface-modified using organosilane compounds. J Membr Sci 182(1):139–149. https://doi.org/10.1016/S0376-7388(00)00559-7
35. Zhuang G-L, Wu C-F, Wey M-Y, Tseng H-H (2021) Impacts of green synthesis process on asymmetric hybrid PDMS membrane for efficient CO_2/N_2 Separation. Membranes 11 (1). https://doi.org/10.3390/membranes11010059
36. Orme CJ, Harrup MK, Luther TA, Lash RP, Houston KS, Weinkauf DH, Stewart FF (2001) Characterization of gas transport in selected rubbery amorphous polyphosphazene membranes. J Membr Sci 186(2):249–256. https://doi.org/10.1016/S0376-7388(00)00690-6
37. Robeson LM (2008) The upper bound revisited. J Membr Sci 320(1):390–400. https://doi.org/10.1016/j.memsci.2008.04.030
38. Kazama S, Teramoto T, Haraya K (2002) Carbon dioxide and nitrogen transport properties of bis(phenyl)fluorene-based cardo polymer membranes. J Membr Sci 207(1):91–104. https://doi.org/10.1016/S0376-7388(02)00112-6
39. Innocenzi P, Abdirashid MO, Guglielmi M (1994) Structure and properties of sol-gel coatings from methyltriethoxysilane and tetraethoxysilane. J Sol-Gel Sci Technol 3(1):47–55. https://doi.org/10.1007/BF00490148
40. Gaabour LH (2017) Spectroscopic and thermal analysis of polyacrylamide/chitosan (PAM/CS) blend loaded by gold nanoparticles. Results Phys 7:2153–2158. https://doi.org/10.1016/j.rinp.2017.06.027
41. Jang J, Park H (2002) Formation and structure of polyacrylamide–silica nanocomposites by sol–gel process. J Appl Polym Sci 83(8):1817–1823. https://doi.org/10.1002/app.10116
42. Jonathan N (1961) The infrared and Raman spectra and structure of acrylamide. J Mol Spectrosc 6:205–214. https://doi.org/10.1016/0022-2852(61)90243-0
43. Pandey P, Chauhan RS (2001) Membranes for gas separation. Prog Polym Sci 26(6):853–893. https://doi.org/10.1016/S0079-6700(01)00009-0
44. Rafiq S, Deng L, Hägg M-B (2016) Role of facilitated transport membranes and composite membranes for efficient CO_2 Capture – A Review. ChemBioEng Rev 3(2):68–85. https://doi.org/10.1002/cben.201500013
45. Bos A, Pünt IGM, Wessling M, Strathmann H (1999) CO_2-induced plasticization phenomena in glassy polymers. J Membr Sci 155(1):67–78. https://doi.org/10.1016/S0376-7388(98)00299-3